SFRP2 supersedes VEGF as an age-related driver of angiogenesis in melanoma, affecting response to anti-VEGF therapy in older patients.

*Mitchell Fane[1,2], *Brett L. Ecker[3], *Amanpreet Kaur[4], Gloria E. Marino[1,2], Gretchen Alicea[1,2], Stephen Douglass[1,2], Yash Chhabra[1,2], Marie R. Webster[5], Andrea Marshall[6], Richard Colling[7], Olivia Espinosa[7], Nicholas Coupe[8], Neera Maroo[8], Leticia Campo[8], Mark R. Middleton[8], Pippa Corrie[8], Xiaowei Xu[9], Giorgos C. Karakousis[3], Ashani T. Weeraratna[1,2]**

[1] Department of Biochemistry and Molecular Biology, Johns Hopkins Bloomberg School of Public Health

[2] Department of Oncology, Sidney Kimmel Cancer Center, Johns Hopkins School of Medicine.

[3] Department of Surgery, University of Pennsylvania, Philadelphia, PA

[4] Department of Engineering and Applied Sciences, University of Pennsylvania, Philadelphia, PA

[5] The Lankenau Institute for Medical Research, Wynnewood PA

[6] Warwick Clinical Trials Unit, University of Warwick, Coventry, UK

[7] Department of Cellular Pathology, Oxford University Hospitals, University of Oxford, Oxford, UK

[8] Department of Oncology, University of Oxford, Oxford, UK

[9] Department of Pathology, University of Pennsylvania, Philadelphia, PA

Keywords: angiogenesis, sFRP2, metastasis, melanoma, aging, microenvironment

***These authors contributed equally**

****To Whom Correspondence Should Be Addressed:**

Ashani T. Weeraratna

aweeraratna@jhu.edu

Department of Biochemistry and Molecular Biology,

Johns Hopkins School of Public Health, and

Department of Oncology,

Johns Hopkins School of Medicine, Baltimore, MD. 21231

Funding: A.T.W, G.A., and G.M., are supported by R01CA174746, and A.T.W., M.F. and S.M.D are supported by R01CA207935. X.X. and A.T.W. are supported by P01 CA114046. X.X., G.K. and A.T.W. are also supported by P50 CA174523. M.R.W. is supported by R00 CA208012-01. ATW is also supported by a Melanoma Research Alliance/ L'Oréal Paris-USA Women in Science Team Science Award, and an Established Investigator Award from the Melanoma Research Foundation, the Wistar Science Discovery Fund, the E.V. McCollum Chair, and a Bloomberg Distinguished Professorship. Core facilities used in this grant are supported by P30CA010815 and P30CA00697356. The AVAST-M study was funded by grants from Cancer Research UK (reference: C7535/A6408 and C2195/A8466). MRM is supported by the NIHR Oxford Biomedical Research Centre. The views expressed are those of the authors and not necessarily those of the NHS, the NIHR or the Department of Health.

Conflict of Interest: The authors declare no potential conflicts of interest

Statement of Translational Relevance: Tumor vascularity is thought to be the conduit to metastatic dissemination. This has led to great interest in targeting angiogenesis, resulting in novel therapies such as bevacizumab (Avastin), an antibody targeted against the vascular endothelial growth factor, VEGF. However, the clinical impact of these drugs on overall survival in melanoma patients is limited, suggesting that VEGF may not be the only factor modulating angiogenesis. Here, we present data which show that VEGF signaling is decreased during aging and superseded by sFRP2, a factor that aggressively guides angiogenesis in older patients. In the presence of sFRP2 therefore, tumors are less responsive to anti-VEGF therapies, which may underlie the lack of efficacy of anti-VEGF therapies in the elderly, while pointing to the fact that younger patients may actually benefit from bevacizumab. Understanding how age-related changes in the tumor microenvironment govern response to targeted therapies can better guide therapeutic options in young vs. aged melanoma patients.

Abstract

Purpose: Angiogenesis is thought to be critical for tumor metastasis. However, inhibiting angiogenesis using antibodies such as bevacizumab (Avastin), has had little impact on melanoma patient survival. We have demonstrated that both angiogenesis and metastasis are increased in older individuals, and therefore sought to investigate if there was an age-related difference in response to bevacizumab, and if so, what the underlying mechanism could be.

Experimental Design: We analyzed data from the AVAST-M trial of 1343 melanoma patients treated with bevacizumab to determine if there is an age-dependent response to bevacizumab. We also examined the age-dependent expression of VEGF and its cognate receptors in melanoma patients, while using syngeneic melanoma animal models to target VEGF in young vs old mice. We also examined the age-related pro-angiogenic factor sFRP2 and if it could modulate response to anti-VEGF therapy.

Results: We show that older patients respond poorly to bevacizumab, whereas younger patients show improvement in both disease-free and overall survival. We find that targeting VEGF does not ablate angiogenesis in an aged mouse model, while sFRP2 promotes angiogenesis *in vitro* and in young mice. Targeting sFRP2 in aged mice successfully ablates angiogenesis, while the effects of targeting VEGF in young mice can be overcome by increasing sFRP2.

Conclusions: VEGF is decreased during aging, thereby reducing response to bevacizumab. Despite the decrease in VEGF, angiogenesis is increased, due to an increase in sFRP2 in the aged tumor microenvironment. These results stress the importance of considering age as a factor for designing targeted therapies.

Introduction

The progression of melanoma to distant metastatic sites increases with age. Age is the single most prognostic factor for patient survival[1], and older patients are at increased risk for the development of frequently incurable visceral metastases[2,3]. However, a mechanistic basis for age-related changes in tumor dissemination that underlie such inferior clinical outcomes is not fully understood[4]. The formation of visceral metastases requires tumor access to the systemic circulation, and in some cancers, low levels of angiogenesis are highly prognostic of distant metastatic-free survival[5,6]. Angiogenesis is accomplished by the recruitment of endothelial cells to the tumor microenvironment, and this is thought to be initiated by tumor cell secretion of factors such as the vascular endothelial growth factor, VEGF. Other factors including platelet derived growth factor (PDGF) and basic fibroblast growth factor (bFGF) are also thought to contribute to VEGF-mediated angiogenesis. Melanoma cells have been shown to increase their production of all of these factors[7,8]. VEGF is thought to be a key factor in the angiogenic pathway, binding to its cognate receptors, and driving signaling that results in endothelial cell proliferation, and migration. However, in melanoma, angiogenesis is complex, and VEGF itself is not thought to be a predictor of poor prognosis in melanoma, as there is no change in the levels of VEGF secreted by metastatic vs primary melanoma lesions[9,10]. Further, while the analyses of human melanoma lesions have shown a strong correlation between angiogenesis and the ability of a melanoma lesion to transition from a radial to a vertical growth phase[11], other indicators of vascularity are not as clear. For example, microvessel density is not thought to correlate to patient prognosis in melanoma in some studies[12], where others show that it does [13,14]. Finally, and further complicating these issues is the fact that melanoma cells themselves can form vascular networks, in a process known as vascular mimicry[15,16].

Despite the complicated landscape of angiogenesis in cancer, bevacizumab, an antibody that is targeted against multiple isoforms of VEGF, has been tested in metastatic cancers of multiple origins, and approved for the treatment of some. Bevacizumab, better known under its trade name Avastin, was tested in melanoma in a clinical trial known as the AVAST-M melanoma trial[17,18]. In this multi-center, randomized, phase III trial, 1343 patients were randomized into those who received Avastin for a year, vs. those who were placed under observation. With a minimum of 5 years follow-up, there were no significant differences for distant-metastasis free survival, or overall survival and only a slight improvement in disease-free intervals. These analyses did not consider age as a variable. Our data show that advanced age of the patient can predict their response to therapy, either in a negative manner, such as an attenuated response to BRAF/ MEK inhibitors[19] or in a positive manner, such as a stronger response to immunotherapy[20,21]. In that context, we wanted to know if the age of the patient could also predict their response to bevacizumab. Further to that, we have previously shown that the aged dermal fibroblast secretome has multiple effects on melanoma progression including increases in genomic instability, resistance to targeted therapy, and metastasis. One of the factors responsible for increased metastatic dissemination is the secreted frizzled-related protein 2 (sFRP2) which is a non-canonical Wnt family member that is elevated in the serum of aged melanoma patients[22]. In cancer models such as breast cancer, sFRP2 stimulates angiogenesis. This function of sFRP2 occurs through a β-catenin-independent pathway, via activated calcineurin/NFAT[23], and has been shown to increase angiogenesis in other cancer models. Targeting sFRP2 with a monoclonal antibody has been shown to overcome angiogenesis in breast cancer models[23], and our own data have shown that angiogenesis in established melanoma tumors in aged mice can also be targeted by antibodies against sFRP2[22], but we have not fully explored the impact of age on angiogenesis. In this study, therefore, we examined the hypothesis that

the age of the melanoma patient could predict response to Avastin, and that the observed age-related resistance to Avastin might be due to the increase in sFRP2 driven angiogenesis.

Results

To determine the effects of aging on angiogenesis, we first stained whole tumor samples from young and aged melanoma patients for CD31, to assess blood vessel density throughout the tumor. We found that the percentage of CD31 coverage within tumors was significantly increased in patients over the age of 65 as compared to patients under the age of 65 (Figure 1A, additional representative staining, Supplemental Figure 1A). Next, we examined neoangiogenesis and lymphangiogenesis in a syngeneic mouse model of melanoma. Yumm1.7 cells[24], derived from the $Braf^{V600E}/Cdkn2a^{-/-}/Pten^{-/-}$ mouse model of melanoma[25] were injected into the dermis of young (8 weeks) or aged (52 weeks) C57/BL6 mice and serial sections of primary tumors were stained for CD105 and LYVE1. Previous studies of ours have shown that CD31 is increased within an aged melanoma mouse tumors[22]; however, while CD31 is a commonly utilized pan-endothelial cell marker, it does not distinguish LYVE-1 positive lymphatic endothelium from CD105-positive blood microvascular endothelium[26]. Moreover, CD105 is thought to be a more specific marker than CD31 for malignancy-associated blood microvasculature[27,28] and has a stronger prognostic significance than traditional vascular markers[29]. In a cohort of genetically identical mice inoculated with identical melanoma cells, tumors in the aged microenvironment showed increased CD105-positive blood microvascular density (Fig. 1B, additional representative staining, Supplemental Figure 1B) with no age-related differences in LYVE1-positive lymphatic vessel density (Fig. 1C). To determine if age-related changes in the fibroblast secretome may account for differences in tumor angiogenesis, adult human dermal

microvascular endothelial cells (HMVECs) were exposed to the conditioned media of dermal fibroblasts from young (<45 years) and aged (>55 years) healthy donors from the Baltimore Longitudinal Study of Aging[30]. The secretome of aged fibroblasts significantly increased the proliferative index of HMVECs (Fig. 1D) as well as the formation of capillary structures in a previously validated *in vitro* tubule formation assay (Fig 1E,F)[31]. In contrast, HMVECs treated with young fibroblast conditioned media or unconditioned media formed less complex capillary structures. Such data support the role of the aged dermal fibroblast secretome as a proangiogenic microenvironment.

To determine if these changes in angiogenesis were driven by classical angiogenic drivers, specifically VEGF, we queried the importance of VEGF signaling in the aged microenvironment. Intriguingly, increased patient age was associated with decreased expression of VEGF (Fig. 2A) as well as its two primary receptors, VEGFR1 (Fig. 2B) and VEGFR2 (Fig. 2C) in an age-stratified analysis of melanoma patient gene expression in TCGA. This decrease in VEGF with age led us to hypothesize that age-related differences in response to bevacizumab (Avastin^{TM}), an anti-VEGF antibody, might exist. We tested this hypothesis by analyzing data from the AVAST-M randomized controlled phase III trial evaluating the role of adjuvant bevacizumab in patients with resected melanoma at high risk of recurrence[17]. Higher VEGF scores in this group also correlated with improved survival, potentially due to the availability of target for the drug (Fig. 2D). Next, we performed a post-hoc trial analysis for the interaction between age and response to treatment. Younger patients who received adjuvant bevacizumab had a significantly longer disease-free interval (age <45 years: HR 0.71, 95% CI 0.53-0.96), while there was no impact of therapy on disease recurrence in older patients (age >65 years: HR 1.00, 95% CI 0.72-1.38) (Fig 2E). Similar patterns of treatment effect trended strongly for the outcome of overall survival as well (Supplemental Fig. 2A). Finally, given that BRAF status has been associated with response to Avastin[18], we examined

the data with an emphasis on BRAF status, and age. We found that the effect of Avastin is significant for young patients harboring the BRAF mutation, although the young patients who were BRAF WT showed a similar non-significant trend. The fact that the data did not reach significance could also be due to the fact that far fewer young patients are BRAF WT. Older patients showed no benefit from bevacizumab regardless of their BRAF status (Supplemental Figure 2B). We also queried the TCGA database for the expression of VEGF and its receptors according to BRAF status and age. We found significant correlations between age and VEGF and most of its receptors, but for the most part, these did not separate out by BRAF status (Supplemental Figure 2C), supporting the observations in Supplemental Figure 2B. We found that the effect of Avastin is significant for young patients who are BRAF mutant, although the young patients who are BRAF WT respond in a similar, albeit non-significant manner. Given that there was no therapeutic benefit for BRAF mutant patients of older age ranges, we hypothesize that age and not BRAF status is the predominant determinant of response to Avastin.

Since increased age-related angiogenesis could not be explained by VEGF changes, and older patients did not appear to benefit from adjuvant bevacizumab, we hypothesized that other factors were driving angiogenesis in the elderly. sFRP2 is an established proangiogenic factor[23,32] and we have previously demonstrated that sFRP2 is an important component of the aged dermal fibroblast secretome, and is associated with increased CD31 staining in tumors in aged mice[22]. The treatment of HMVECs with recombinant sFRP2 was sufficient to increase cell proliferation (Fig. 3A) and its addition to young conditioned media increased capillary formation *in vitro* to levels observed with treatment with aged conditioned media (Fig. 3B,C). HMVEC treatment with aged conditioned media and a neutralizing α-SFRP2 antibody was sufficient to inhibit *in vitro* angiogenesis (Fig 3B, lower panels).

These data suggested that sFRP2 may take over as the predominant pro-angiogenic factor during aging. To further support this, analysis of melanoma samples in the TCGA data base demonstrates that there is a positive association between CD105 and sFRP2, while VEGF expression inversely correlates with CD105 expression (Fig. 3D,E. Further, we observed that sFRP2 is increased in ulcerated tumors, which have large amounts of blood vessels, whereas VEGF showed no such correlation to ulceration (Supplemental Fig 3A, B). We assessed the impact of sFRP2 on neo-angiogenesis *in vivo*, specifically by assessing CD105 staining. We injected Yumm1.7 cells into the dermis of young (8 weeks) C57/BL6 mice treated with recombinant sFRP2 (rsFRP2) (200ng/ml, tail vein, twice weekly) or PBS control. In parallel, we also injected Yumm1.7 cells into the dermis of aged (52 weeks) C57/BL6 mice treated with anti-sFRP2 antibody (1mg/kg, tail vein, once weekly) or with IgG2aκ control. Subsequently, we stained these tumors for intra-tumoral CD105-positive microvascular density, which was significantly greater in young mice treated with rsFRP2 (Fig. 3F) with no difference in lymphatic vessel density (Fig. 3G). Neutralizing sFRP2 in aged mice was sufficient to reduce CD105-positive microvascular density, without any quantifiable changes in lymphatic vessel density. Notably, there was no difference in tumor size with rsFRP2 or α-sFRP2 treatment (Supplemental Fig. 3C,D), nor increased human melanoma cell proliferation with rsFRP2 treatment *in vitro* (Supplemental Fig. 3E), supporting a selective effect on endothelial and not melanoma cell proliferation, and excluding any potential bias between tumor size and vascularity. Finally, we also confirm previous data showing that treating young mice with recombinant sFRP2 drives melanoma cell metastasis from the skin to the lung, and that inhibiting sFRP2 in aged mice inhibits metastatic progression to the lung (Supplemental Fig. 3F,G). Together these data showed that the observed age-related increase in angiogenesis was likely due to sFRP2.

To test the hypothesis that sFRP2 superseded VEGF as the predominant angiogenic factor during aging, we examined serial sections of primary Yumm1.7 allografts from untreated young or aged C57/BL6 mice for their VEGF and sFRP2 status. As observed with the human data, increasing age led to a decrease in VEGF expression, and we also observed a parallel increase in sFRP2 expression (Figure 4A,B). To test if increased sFRP2 could impact response to anti-VEGF therapies, we treated young mice with an antibody against VEGF-A (bevacizumab is species specific and cannot neutralize murine VEGF-A[33]) in the presence and absence of sFRP2. Anti-VEGF reduced angiogenesis in mouse tumors in young mice in vivo; however, when administered in the presence of rsFRP2, there was no reduction in angiogenesis, and indeed blood vessel density was increased, just as it is in the presence of sFRP2 alone (Figure 4C,D, additional representative staining in Supplemental Figure 4). Tumor size was unaffected by treatment (Figure 4E), and there was little toxicity with the treatments (Fig. 4F). This confirmed our hypothesis that when sFRP2 levels increase, as they do in aging, anti-VEGF therapy is no longer effective, and provides a basis for the observed lack of benefit from adjuvant bevacizumab in older patients recruited to the AVAST-M trial. Overall, our data suggest that angiogenesis is increased in the aged tumor microenvironment, but that this angiogenesis is an sFRP2 rather than VEGF driven process. Since VEGF is no longer the predominant angiogenic factor in older patients, targeting this pathway may have less impact in older versus younger patients.

Discussion

Angiogenesis in melanoma is complex, and we show in this study that age-related changes in the tumor microenvironment further limit the efficacy of current therapies targeting angiogenesis. We have shown that angiogenesis and growth are uncoupled in melanoma, such that tumors in aged mice have more angiogenesis, and

metastasize at much great rates, but actually grow far more slowly than tumors in young mice[22]. This may be due to the fact that the factors that drive angiogenesis in aging (e.g., sFRP2) also increase other factors such as Wnt5A which we have shown previously is a powerful suppressor of growth and proliferation, and promotes a slow-cycling phenotype in melanoma allowing cells to resist therapy[34]. Angiogenesis thus becomes only one of a myriad of changes wrought by the aged microenvironment, and we have shown that these changes encompass everything from biophysical changes[35] to immune microenvironment changes[21] to changes in lipid secretion and uptake[19]. In addition to sFRP2, we have found other factors in the secretome of aged fibroblasts that may also have an impact on angiogenesis. These include RARRES1 and CLU. Intriguingly, RARRES1 has been shown to inhibit VEGF[36], further supporting our theory that VEGF levels are decreased during aging. Whether or not this affects sFRP2 levels, or whether sFRP2 can induce RARRES1 remains an open question, and a topic of further study. We also identified CLU as elevated in the aged secretome. This first seemed counter-intuitive as CLU or clusterin, has been shown to increase angiogenesis in ovarian cancer, however, the role of CLU is dependent upon VEGF[37]. It is possible that the increase in CLU is a futile attempt to compensate for VEGF decreases. Therefore, the significance of clusterin in age and sFRP2-induced angiogenesis is somewhat unclear. The roles of both of RARRES and CLU, and their potential regulation by sFRP2 and/ or other age-related factors remain interesting areas to pursue.

One area that we did not explore in the current study is the important area of blood vessel integrity and pericyte coverage. Helfrich et al[38] have shown that increased pericyte coverage can confer resistances to anti-VEGF treatment strategies, and this is consistent with our observed increases in CD31 staining in aged human patients. This study used the MT/RET mouse model of melanoma to uncover the changes that occur in the stabilization of blood vessels, and intriguingly, this mouse model is an excellent

model in which to study aging-related changes. MT-RET transgenic mice are engineered to express the human ret transgene in melanocytes controlled by the mouse metallothionein-I promoter-enhancer[39]. These mice are reported to spontaneously develop melanomas metastasizing to lymph nodes, lungs, brain, kidney and spleen. This process involves the development of skin melanosis (100% just after birth), benign melanocytic tumors (100% after 6 months), and metastatic melanoma (65-70% in mice 18 months old). The Helfrich study examined pericyte coverage in lesions with high vs low levels of angiogenesis, but it is unclear whether these studies took into account the age at which the highly angiogenic versus less angiogenic tumors developed, and if there was an age-related component of angiogenesis in this model. It is important to note that in this study, they, like us, observed that angiogenesis was uncoupled from tumor size.

While currently available anti-angiogenic therapies target the VEGF pathways, age-dependent loss in VEGF, in tandem with increases in alternative angiogenic pathways, such as sFRP2, may limit efficacy of Bevacizumab in older melanoma patients, but could potentially still be an appropriate treatment in young patients. The AVAST-M trial demonstrated that adjuvant bevacizumab improved the disease-free interval compared with observation alone in the overall recruited patient population, although this early benefit did not translate to an overall survival gain. The trial was not designed to adjust for patient age in the randomization process, thus these post-hoc data must be interpreted with caution. However, there does appear to be a striking association between patient age and risk of relapse after adjuvant bevacizumab. Additional data also suggest that using bevacizumab in conjunction with immunotherapy (specifically ipilimumab) results in an improved immune microenvironment[40], potentially increasing response to immunotherapy. Given our data and others showing that older

patients already have an enhanced response to immunotherapy, this observation warrants further investigation.

It remains to be determined whether sFRP2 can be targeted in human melanoma patients. Alternatively, drug therapies targeting the downstream mediators of sFRP2 may be additional avenues for exploration. The aged secretome is characterized by disturbances in multiple proteins including increases in Wnt5A, which can also activate NFAT via CAMKII/calcineurin pathways[41,42], suggesting sFRP2 and Wnt5A may work in concert during aging to increase angiogenesis. In fact, similar increases in angiogenesis were observed following treatment with rWnt5a *in vitro* (Supplemental Fig. 5A) and in Wnt5a-overexpressing Yumm1.7 tumors (Supplemental Fig. 5B). As calcineurin inhibitors (e.g., tacrolimus) have already been approved for human use, this may be a preferred strategy for inhibiting age-related angiogenesis by blocking a convergence of NFAT-driven mechanisms, and indeed have been suggested before[43]. In conclusion, the aged tumor microenvironment promotes hematogenous melanoma dissemination, where loss of VEGF is offset with overexpression of proangiogenic sFRP2. Together, these data provide therapeutic rationale to consider patient age in decisions regarding selection of therapy.

Methods

Cell lines and culture conditions

Dermal fibroblast cell lines were obtained from Biobank at Coriell Institute for Medical Research. The fibroblasts were cultured in DMEM (Invitrogen) supplemented with 10% FCS and 4mM L-glutamine. HMVEC-dBlAd cells were obtained from Lonza and cultured in EGM-2MV media (CC-3202, Lonza). Murine Yumm1.7 melanoma cells were cultured in DMEM supplemented with 10%FCS and 4mM L-glutamine. WM35 melanoma cells were maintained in in MCDB153 (Sigma)/L-15 (Cellgro; 4:1 ratio)

supplemented with 2% FBS and 1.6 mmol/L $CaCl_2$ (tumor growth media). All the cell lines were cultured at 37°C in 5% CO_2. Short tandem repeat profiling was done for melanoma cells and compared against our internal control of over 200 melanoma cell lines as well as control lines such as HeLa and 293T and the results are available upon request. Mycoplasma testing was carried out using a Lonza MycoAlert assay at the University of Pennsylvania Cell Center Services.

Cellular Proliferation assay

In a 24 well plate, 5000 cells were plated in triplicate per day of measurement. Cells were treated with recombinant sFRP2 (200ng/ml, #6838-FR, R&D) without any replacement of addition of fresh medium. Every 2-3 days, cells were counted using hemocytometer and the total cell number in the well was recorded. Graphs were plotted using percent proliferation based on day 0.

Tubule formation assay

HMVEC-dBlAd cells were purchased from Lonza as stated. Cells were thawed and allowed to grow for two passages before the assay was performed as previously described[44]. Briefly, 48 well plates were covered with 90µl Matrigel (concentration >10mg/ml; BD Biosciences, #354234) and allowed to solidify at room temperature for 30 minutes. HMVEC cells were aliquoted at 50,000 cells per well, resuspended in 400µl of media and added dropwise to each well. Young and aged media were concentrated at ~10x using 3000 Da MWCO filters (UFC900324, Amicon, EMD Millipore) and reconstituted to 1x with DMEM containing 10% FCS. Reagents were purchased from rsFRP2 (200ng/ml, 6838-FR, R&D Systems), Wnt5a (200ng/ml, 645-WN, R&D Systems), anti-sFRP2 neutralizing antibody (15µg/ml, MABC539, EMD Millipore). bFGF

at 35ng/ml is used as positive control. Plates were incubated at 37°C for 12-18 hours. Tubules will start to appear at 10-12 hours and start to contract over time. Images were taken at various intervals to determine optimal tubule formation.

Immunohistochemistry

Patient samples were collected under IRB exemption approval (protocol EX21205258-1). FFPE sections were deparaffinized using xylene followed by rehydration through series of alcohol washes and finally PBS. Heat-mediated antigen retrieval was performed using citrate based retrieval buffer (Vector Labs, H-3300). Samples were blocked in peroxide blocking buffer (Thermo Scientific), followed by protein block (Thermo Scientific) and incubated in appropriate antibody at 4°C overnight in a humidified chamber. Following day, samples were washed and incubated with a biotinylated secondary antibody (Thermo Scientific) followed by Streptavidin-HRP incubation. Samples were then washed in PBS and incubated in 3-amino-9-ethyl-1-carboazole (AEC) chromogen and counterstained with Mayer's hematoxylin, rinsed in dH_2O and mounted in Aquamount. For mouse samples to be incubated with mouse antibodies, samples were blocked for an additional hour with mouse on mouse block (MKB-2213, Vector Labs). Primary antibodies used were as follows: CD105/Endoglin (1:100, MAB1320, R&D Systems), Lyve-1 (1:50, ab14917, abcam). sFRP2 (1:100, ab137560, abcam), VEGF (human: 1:100, M727329-8, DAKO; mouse: 1:50, sc7269, Santa Cruz Biotechnology), CD31 (1:100, GA61061-2, DAKO), mCherry (1:500, NBP2-25157, Novus Biologicals), biotinylated Wnt5A (500 ng/mL, BAF645, R&D Systems).

Immunofluorescence

Samples were fixed in 4% paraformaldehyde for 20 minutes followed by 1 hour treatment with blocking buffer (0.2% each of triton-x, BSA, gelatin and casein and 0.02%

sodium azide). Cells were incubated in primary antibody and incubated overnight at 4°C. Following day, cells were washed in PBS and incubated with appropriate secondary antibodies (Alexa fluor series, Invitrogen, 1:2000) at room temperature for 1 hour. Cells were washed in PBS, incubated with DAPI (Invitrogen, 1:10,000) and mounted in Prolong Gold anti-fade reagent (Invitrogen). Images were captured on a Leica TCS SPII scanning laser confocal system. Primary antibodies used were as follows: Ki67 (1:400, #9027, Cell Signaling), sFRP2 (1:100, MAB6838, R&D Systems), biotinylated Wnt5A (500 ng/mL, BAF645, R&D Systems).

In vivo allograft assay

All animal experiments were approved by the Institutional Animal Care and Use Committee (IACUC) (IACUC #112503X_0, IACUC #112510X_0) and were performed in an Association for the Assessment and Accreditation of Laboratory Animal Care (AAALAC) accredited facility. Yumm1.7 (1×10^5 cells) overexpressing mCherry or mCherry-Wnt5a were injected subcutaneously into aged (52 weeks) and young (8 weeks old) C57/BL6 mice (#556, Charles River). Mice were treated as follows with rsFRP2 (200ng/ml, tail vein, twice weekly), anti-sFRP2 antibody (1mg/kg, tail vein, once weekly), anti-VEGF (1mg/kg, tail vein, once weekly) or PBS, IgG2aκ and goat IgG as control. Tumor sizes were measured every 3-4 days using digital calipers, and tumor volumes were calculated using the following formula: volume = 0.5 x (length x width^2). Time-to-event (survival) was determined by a 5-fold increase in baseline volume (~1000 mm^3) and was limited by the development of skin necrosis. Mice were euthanized and primary tumors and lungs harvested. Half of the tissue was embedded in paraffin and half in optimal cutting temperature compound (O.C.T, Sakura, Japan City) and flash frozen for sectioning. Lungs were sectioned and stained with mCherry (NBP2-25157, Novus Biologicals) to determine melanoma metastasis. All reagents injected in live mice were

tested for endotoxin levels at University of Pennsylvania Cell Center Services using The Associates of Cape Cod LAL test.

TCGA database analysis

The RNAseq and Clinical dataset for skin cutaneous melanoma[45] was downloaded from The Cancer Genome Atlas (TCGA; http://cancergenome.nih.gov/). Normalized mRNA expression was analyzed by quartiles. Patient ages were grouped into categories (<45, 45-65, and >65 years). High vs low categories (sFRP2 and VEGFa) were stratified based on the 25 percentile of high or low expressing tumor samples.

Lentiviral production and infection

Wnt5a overexpression plasmid was prepared by cloning Wnt5a from pLNCX2 plasmid published previously[34] into lentiviral pLU-MCS-IRES-mCherry plasmid. Sequencing based verification of all plasmids was performed at the Genomics facility at The Wistar Institute. Lentiviral production was performed according to the protocol suggested by the Broad Institute. Briefly, 293T cells are plated at 70% confluency and co-transfected with shRNA plasmid and the lentiviral packaging plasmids (pCMV-dR8.74psPAX2, pMD2.G). pLKO.1 empty vector was used as a control. For transduction, cells were treated with lentivirus overnight and allowed to recover for 24 hours before selection using puromycin (1µg/ml).

Statistical analyses

For *in vitro* studies, a Student t test or Wilcoxon rank-sum test (Mann–Whitney) was performed for two-group comparison. Estimate of variance was performed, and parameters for the t test were adjusted accordingly using Welch's correction. ANOVA or Kruskal–Wallis test with post-hoc Bonferroni's or Holm–Sidak's adjusted P values was

used for multiple comparisons. For in vivo studies, repeated measures ANOVA was calculated between samples. The Holm–Sidak correction was performed. Kaplan-Meier and Cox regression was utilized for univariate and multivariate survival analyses, respectively For other experiments, Graphpad/Prism8 was used for plotting graphs and statistical analysis. Data was represented as ±SEM. Significance was designated as follows: *, $P < 0.05$; **, $P < 0.01$; and ***, $P < 0.001$.

Authors' contributions: conception/design (BL Ecker, A Kaur, MR Middleton, GC Karakousis, AT Weeraratna); data acquisition (BL Ecker, A Kaur, M Fane, MR Webster, S Douglass, Y Chhabra, GE Marino, GM Alicea, A Marshall, R Colling, P. Corrie, O Espinosa, N Coupe, N Maroo, L Campo, X Xu); data interpretation (all authors); drafting (BL Ecker, AT Weeraratna, M Fane); critical revisions (all authors); final approval (all authors)

Declaration of interests: none

References

1. Balch CM, Gershenwald JE, Soong SJ, et al. Final version of 2009 AJCC melanoma staging and classification. *J Clin Oncol.* 2009;27(36):6199-6206.
2. Lasithiotakis K, Leiter U, Meier F, et al. Age and gender are significant independent predictors of survival in primary cutaneous melanoma. *Cancer.* 2008;112(8):1795-1804.
3. Balch CM, Soong SJ, Gershenwald JE, et al. Age as a prognostic factor in patients with localized melanoma and regional metastases. *Ann Surg Oncol.* 2013;20(12):3961-3968.
4. Fane M, Weeraratna AT. How the ageing microenvironment influences tumour progression. *Nat Rev Cancer.* 2020;20(2):89-106.
5. Kashani-Sabet M, Sagebiel RW, Ferreira CM, Nosrati M, Miller JR, 3rd. Tumor vascularity in the prognostic assessment of primary cutaneous melanoma. *J Clin Oncol.* 2002;20(7):1826-1831.
6. Neitzel LT, Neitzel CD, Magee KL, Malafa MP. Angiogenesis correlates with metastasis in melanoma. *Ann Surg Oncol.* 1999;6(1):70-74.
7. Adamcic U, Skowronski K, Peters C, Morrison J, Coomber BL. The effect of bevacizumab on human malignant melanoma cells with functional VEGF/VEGFR2 autocrine and intracrine signaling loops. *Neoplasia.* 2012;14(7):612-623.
8. Shih IM, Herlyn M. Autocrine and paracrine roles for growth factors in melanoma. *In Vivo.* 1994;8(1):113-123.
9. Mabeta P. Paradigms of vascularization in melanoma: Clinical significance and potential for therapeutic targeting. *Biomed Pharmacother.* 2020;127:110135.
10. Straume O, Akslen LA. Importance of vascular phenotype by basic fibroblast growth factor, and influence of the angiogenic factors basic fibroblast growth factor/fibroblast growth factor receptor-1 and ephrin-A1/EphA2 on melanoma progression. *Am J Pathol.* 2002;160(3):1009-1019.
11. Erhard H, Rietveld FJ, van Altena MC, Brocker EB, Ruiter DJ, de Waal RM. Transition of horizontal to vertical growth phase melanoma is accompanied by induction of vascular endothelial growth factor expression and angiogenesis. *Melanoma Res.* 1997;7 Suppl 2:S19-26.
12. Perivoliotis K, Ntellas P, Dadouli K, Koutoukoglou P, Ioannou M, Tepetes K. Microvessel Density in Patients with Cutaneous Melanoma: An Up-to-Date Systematic Review and Meta-Analysis. *J Skin Cancer.* 2017;2017:2049140.
13. Depasquale I, Thompson WD. Microvessel density for melanoma prognosis. *Histopathology.* 2005;47(2):186-194.
14. Pastushenko I, Vermeulen PB, Carapeto FJ, et al. Blood microvessel density, lymphatic microvessel density and lymphatic invasion in predicting melanoma metastases: systematic review and meta-analysis. *Br J Dermatol.* 2014;170(1):66-77.
15. Hendrix MJ, Seftor EA, Seftor RE, Chao JT, Chien DS, Chu YW. Tumor cell vascular mimicry: Novel targeting opportunity in melanoma. *Pharmacol Ther.* 2016;159:83-92.
16. Zhang Z, Imani S, Shasaltaneh MD, et al. The role of vascular mimicry as a biomarker in malignant melanoma: a systematic review and meta-analysis. *BMC Cancer.* 2019;19(1):1134.
17. Corrie PG, Marshall A, Dunn JA, et al. Adjuvant bevacizumab in patients with melanoma at high risk of recurrence (AVAST-M): preplanned interim results from

a multicentre, open-label, randomised controlled phase 3 study. *Lancet Oncol.* 2014;15(6):620-630.
18. Corrie PG, Marshall A, Nathan PD, et al. Adjuvant bevacizumab for melanoma patients at high risk of recurrence: survival analysis of the AVAST-M trial. *Ann Oncol.* 2018;29(8):1843-1852.
19. Alicea GM, Rebecca VW, Goldman AR, et al. Changes in Aged Fibroblast Lipid Metabolism Induce Age-dependent Melanoma Cell Resistance to Targeted Therapy Via the Fatty Acid Transporter FATP2. *Cancer Discov.* 2020.
20. Jain V, Hwang WT, Venigalla S, et al. Association of Age with Efficacy of Immunotherapy in Metastatic Melanoma. *Oncologist.* 2020;25(2):e381-e385.
21. Kugel CH, 3rd, Douglass SM, Webster MR, et al. Age Correlates with Response to Anti-PD1, Reflecting Age-Related Differences in Intratumoral Effector and Regulatory T-Cell Populations. *Clin Cancer Res.* 2018;24(21):5347-5356.
22. Kaur A, Webster MR, Marchbank K, et al. sFRP2 in the aged microenvironment drives melanoma metastasis and therapy resistance. *Nature.* 2016;532(7598):250-254.
23. Courtwright A, Siamakpour-Reihani S, Arbiser JL, et al. Secreted frizzle-related protein 2 stimulates angiogenesis via a calcineurin/NFAT signaling pathway. *Cancer Res.* 2009;69(11):4621-4628.
24. Meeth K, Wang JX, Micevic G, Damsky W, Bosenberg MW. The YUMM lines: a series of congenic mouse melanoma cell lines with defined genetic alterations. *Pigment Cell Melanoma Res.* 2016;29(5):590-597.
25. Dankort D, Curley DP, Cartlidge RA, et al. Braf(V600E) cooperates with Pten loss to induce metastatic melanoma. *Nat Genet.* 2009;41(5):544-552.
26. Podgrabinska S, Braun P, Velasco P, Kloos B, Pepper MS, Skobe M. Molecular characterization of lymphatic endothelial cells. *Proc Natl Acad Sci U S A.* 2002;99(25):16069-16074.
27. Dallas NA, Samuel S, Xia L, et al. Endoglin (CD105): a marker of tumor vasculature and potential target for therapy. *Clin Cancer Res.* 2008;14(7):1931-1937.
28. Minhajat R, Mori D, Yamasaki F, Sugita Y, Satoh T, Tokunaga O. Organ-specific endoglin (CD105) expression in the angiogenesis of human cancers. *Pathol Int.* 2006;56(12):717-723.
29. Tanaka F, Otake Y, Yanagihara K, et al. Correlation between apoptotic index and angiogenesis in non-small cell lung cancer: comparison between CD105 and CD34 as a marker of angiogenesis. *Lung Cancer.* 2003;39(3):289-296.
30. Park HW. Biological aging and social characteristics: gerontology, the Baltimore city hospitals, and the national institutes of health. *J Hist Med Allied Sci.* 2013;68(1):49-86.
31. DeCicco-Skinner KL, Henry GH, Cataisson C, et al. Endothelial cell tube formation assay for the in vitro study of angiogenesis. *J Vis Exp.* 2014(91):e51312.
32. Siamakpour-Reihani S, Caster J, Bandhu Nepal D, et al. The role of calcineurin/NFAT in SFRP2 induced angiogenesis--a rationale for breast cancer treatment with the calcineurin inhibitor tacrolimus. *PLoS One.* 2011;6(6):e20412.
33. Yu L, Wu X, Cheng Z, et al. Interaction between bevacizumab and murine VEGF-A: a reassessment. *Invest Ophthalmol Vis Sci.* 2008;49(2):522-527.
34. Webster MR, Fane ME, Alicea GM, et al. Paradoxical Role for Wild-Type p53 in Driving Therapy Resistance in Melanoma. *Mol Cell.* 2020;77(3):633-644 e635.

35. Kaur A, Ecker BL, Douglass SM, et al. Remodeling of the Collagen Matrix in Aging Skin Promotes Melanoma Metastasis and Affects Immune Cell Motility. *Cancer Discov.* 2019;9(1):64-81.
36. Roy A, Ramalinga M, Kim OJ, et al. Multiple roles of RARRES1 in prostate cancer: Autophagy induction and angiogenesis inhibition. *PLoS One.* 2017;12(7):e0180344.
37. Fu Y, Lai Y, Wang Q, et al. Overexpression of clusterin promotes angiogenesis via the vascular endothelial growth factor in primary ovarian cancer. *Mol Med Rep.* 2013;7(6):1726-1732.
38. Helfrich I, Scheffrahn I, Bartling S, et al. Resistance to antiangiogenic therapy is directed by vascular phenotype, vessel stabilization, and maturation in malignant melanoma. *J Exp Med.* 2010;207(3):491-503.
39. Kato M, Takahashi M, Akhand AA, et al. Transgenic mouse model for skin malignant melanoma. *Oncogene.* 1998;17(14):1885-1888.
40. Hodi FS, Lawrence D, Lezcano C, et al. Bevacizumab plus ipilimumab in patients with metastatic melanoma. *Cancer Immunol Res.* 2014;2(7):632-642.
41. Ando F, Sohara E, Morimoto T, et al. Wnt5a induces renal AQP2 expression by activating calcineurin signalling pathway. *Nat Commun.* 2016;7:13636.
42. Stefater JA, 3rd, Rao S, Bezold K, et al. Macrophage Wnt-Calcineurin-Flt1 signaling regulates mouse wound angiogenesis and repair. *Blood.* 2013;121(13):2574-2578.
43. Courtwright A, Siamakpour-Reihani S, Arbiser JL, et al. Secreted frizzle-related protein 2 stimulates angiogenesis via a calcineurin/NFAT signaling pathway. *Cancer research.* 2009;69(11):4621-4628.
44. Arnaoutova I, Kleinman HK. In vitro angiogenesis: endothelial cell tube formation on gelled basement membrane extract. *Nat Protoc.* 2010;5(4):628-635.
45. Cancer Genome Atlas N. Genomic Classification of Cutaneous Melanoma. *Cell.* 2015;161(7):1681-1696.

Figures and Legends

Figure 1. Aging increases angiogenesis in melanoma. A. Representative CD31 staining in young and aged human melanoma samples (100X, n=28, under 65yo; n=12,over 65yo). B. Representative CD105 immunohistochemistry of Yumm 1.7 melanoma tumors five weeks following intradermal injection in young (8 weeks) and aged (52 weeks) C57/BL6 mice (n=10/arm; magnification 400x),with quantification of intratumoral blood vessel density shown in the graph; C. Representative LYVE1 immunohistochemistry of Yumm 1.7 melanoma tumors five weeks following intradermal injection in young (8 weeks) and aged (52 weeks) C57/BL6 mice (n=10/arm; magnification 400x), with quantification of intratumoral lymphatic vessel density shown in the graph. D. HMVECs were treated for 24 hours with conditioned media from young or aged dermal fibroblasts and stained for Ki67 by immunofluorescence, with quantification of Ki67-positive HMVECs per high power field (HPF) shown in the graph; E. Representative light-field images of HMVEC tubule formation following treatment with conditioned media from young or aged dermal fibroblasts or unconditioned fibroblast media; F. Quantification of number of tubule nodes per high power field.

Figure 2. Relationship of VEGF to age and response to bevacizumab. A. Age-stratified TCGA analysis of VEGFA mRNA expression of cutaneous melanoma (n=465); **B**. Age-stratified TCGA analysis of VEGFR1 (FLT1) mRNA expression of cutaneous melanoma (n=465); **C**. Age-stratified TCGA analysis of VEGFR2 (KDR) mRNA expression of cutaneous melanoma (n=465). **D.** Correlation of high vs. low VEGF expression to survival in AVASTM patients; **E**, Age-stratified analysis of disease-free survival in melanoma patients randomized to bevacizumab therapy or observation (n=1,324).

Figure 3. sFRP2 increases angiogenesis during aging. **A**. Proliferation assay of HMVECs grown with standard growth media with the addition of rSFRP2 (200 ng/mL) or PBS control; **p<0.01; ***p<0.001, ****p<0.0001; **B**. Representative light-field images of HMVEC tubule formation following treatment with conditioned media from young fibroblasts with rSFRP2 or aged fibroblasts with neutralizing α-SFRP2 antibody; **C**. Quantification of number of tubule nodes per high power field in B. **D**. Quantification of CD105 positivity in sFRP2 low vs. high tumor in TCGA samples. **E**. Quantification of CD105 positivity in VEGF low vs. high tumor in TCGA samples. **F**. Representative CD105 immunohistochemistry of primary Yumm 1.7-mcherry murine tumors in young C57BL/6 mice treated with PBS or rSFRP2, and aged mice treated with α-SFRP2 antibody or IgG2aκ control and quantification of CD105-positive vessel density; **G**. Representative LYVE1 immunohistochemistry of primary Yumm 1.7-mcherry murine tumors in young C57BL/6 mice treated with PBS or rSFRP2, and aged mice treated with α-SFRP2 antibody or IgG2aκ control and quantification of LYVE1-positive vessel density.

Figure 4: sFRP2 treatment overcomes response to anti-VEGF. A. Representative immunohistochemistry of VEGF and sFRP2 staining in tumors in young and aged mice; **B**. Quantification of staining in A, based on the H-score calculated by percent of tumor positive, and intensity of stain. **C**. Representative CD105 immunohistochemistry of primary Yumm 1.7 mcherry murine tumors in young C57BL/6 mice treated with PBS or rsFRP2, in the presence of the anti-VEGFA antibody, or an IgG control. **D**. Quantification of staining in C. **E**. Yumm 1.7 cells were implanted in mice and then mice were treated

with antibody treatments as indicated, and tumor growth was measured. **F.** Mouse weight in grams after indicated treatments, beginning 12 days after tumor inoculation.

Supplemental Figure Legends

Supplemental Figure 1. Representative immunohistochemistry images. A. Representative images of CD31 staining in young and aged human melanoma patients. **B.** Representative images of CD105 staining in young and aged mouse tumors.

Supplemental Figure 2. Avastin Response in Patients. **A**. Age-stratified analysis of overall survival in melanoma patients randomized to bevacizumab therapy or observation (n=1,324). **B.** Forest plot showing the association between BRAF, age and treatment response for disease free interval in Avastin treated patients. **C**. Expression of VEGF and its receptors according to BRAF status and age using TCGA data.

Supplemental Figure 3: sFRP2 treatment does not affect tumor growth, but does increase invasion. **A**. Quantification of sFRP2 expression in ulceration positive vs negative tumors in TCGA samples. **B**. Quantification of VEGF expression in ulceration positive vs negative tumors in TCGA samples. **C**. Tumor growth curves of Yumm1.7-mCherry murine tumors in young C57/BL6 mice treated with PBS or rSFRP2; **D**. Tumor growth curves of Yumm1.7-mCherry murine tumors in aged C57/BL6 mice treated with α-SFRP2 antibody or IgG2aκ control; **E**. Proliferation assay of WM35 melnaoma cells grown with standard growth media with the addition of rsFRP2 (200ng/mL) or PBS control. **F**. mCherry staining of Yumm1.7-mCherry cells in mouse lung that metastasized from subcutaneous injection in young mice treated with either PBS or rsFRP2 or **G**. aged mice treated with IgG control, or anti-sFRP2 antibody.

Supplemental Figure 4. Representative images of CD105 staining in young mice treated with anti-VEGF, rsFRP2, or the combination. Representative CD105 immunohistochemistry of primary Yumm 1.7 mcherry murine tumors in young C57BL/6 mice treated with PBS or rsFRP2, in the presence of the anti-VEGFA antibody, or an IgG control as indicated.

Supplemental Figure 5. Wnt5A expression can also increase angiogenesis. A. Representative light-field images of HMVEC tubule formation following treatment with young fibroblast conditioned media and PBS or rWnt5a (200ng/mL); **B**. Quantification of number of tubule nodes per high power field; **C**. Representative CD105 immunohistochemistry of control or Wnt5a-overexpressing Yumm1.7 tumors in young C57/BL6 mice (n=4 per arm); **D**. Quantification of CD105-positive vessels/HPF.

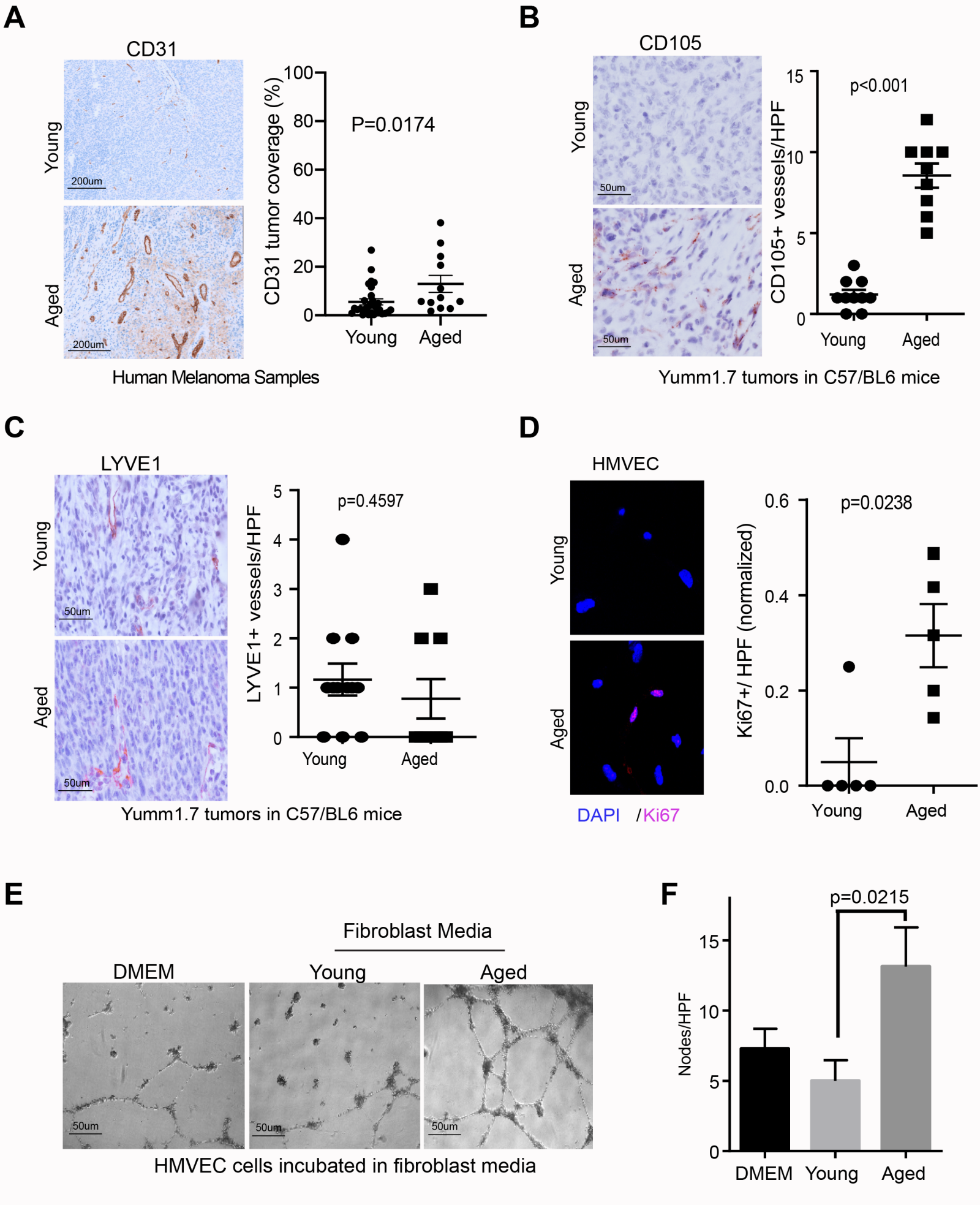
A
CD31
Young
Aged
200um
200um
CD31 tumor coverage (%)
100
80
60
40
20
0
P=0.0174
Young
Aged
Human Melanoma Samples
B
CD105
Young
Aged
50um
50um
CD105+ vessels/HPF
15
10
5
0
p<0.001
Young
Aged
Yumm1.7 tumors in C57/BL6 mice
C
LYVE1
Young
Aged
50um
50um
LYVE1+ vessels/HPF
5
4
3
2
1
0
p=0.4597
Young
Aged
Yumm1.7 tumors in C57/BL6 mice
D
HMVEC
Young
Aged
DAPI /Ki67
Ki67+/ HPF (normalized)
0.6
0.4
0.2
0.0
p=0.0238
Young
Aged
E
Fibroblast Media
DMEM
Young
Aged
50um
50um
50um
HMVEC cells incubated in fibroblast media
F
p=0.0215
Nodes/HPF
15
10
5
0
DMEM
Young
Aged

Figure 1

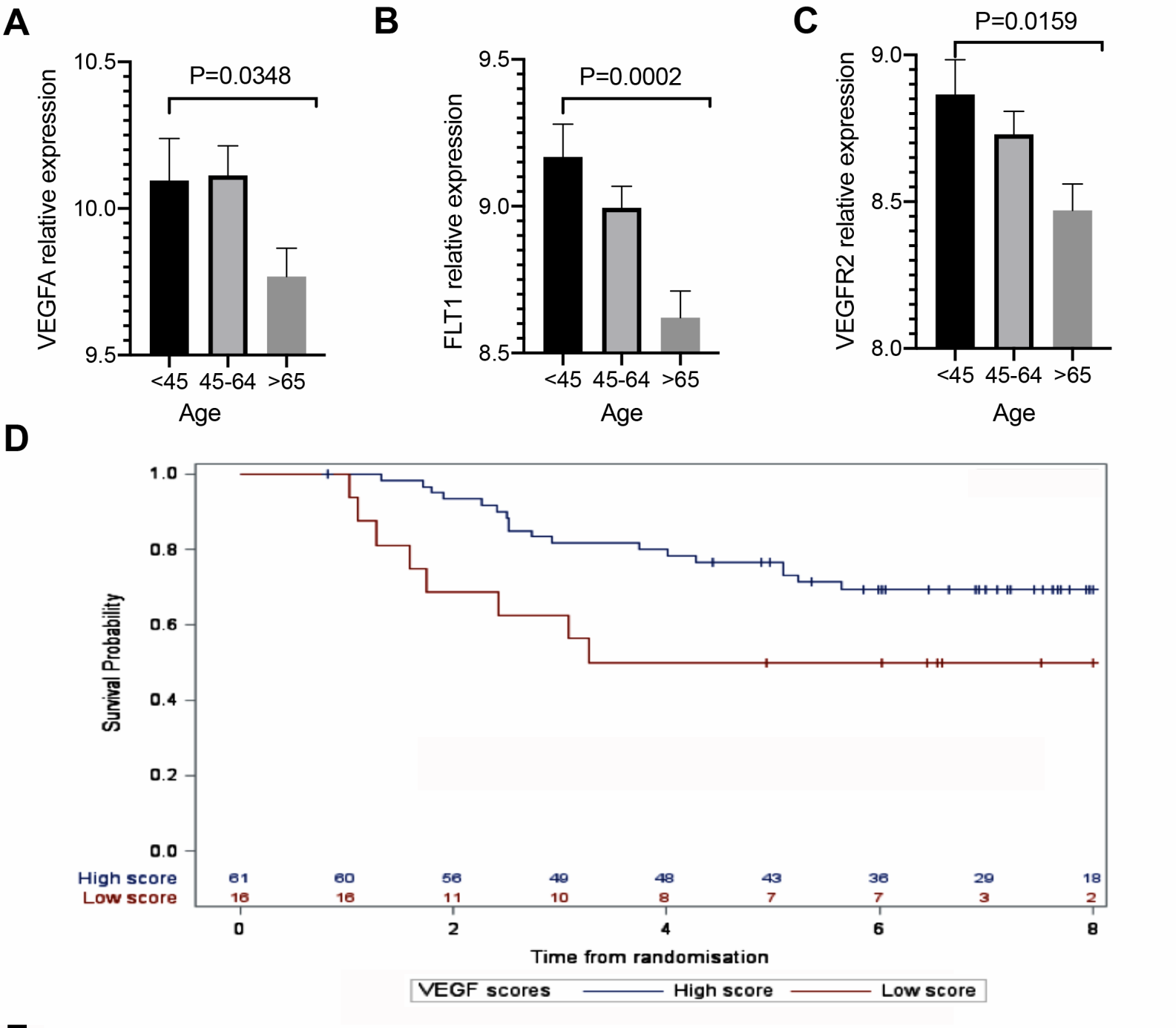

E

	Events/Patients Treatment	Obs	Treatment events (O-E)	Var	*Hazard Ratio & CI (Treatment : Obs)	*HR & CI (Treatment : Obs)
Age						
<45 years	74/168 (44.0%)	101/189 (53.4%)	-14.9	43.7		0.71 (0.53, 0.96)
45-65 years	182/367 (49.6%)	189/334 (56.6%)	-17.0	92.2		0.83 (0.68, 1.02)
65 years	66/117 (56.4%)	82/149 (55.0%)	-0.1	36.5		1.00 (0.72, 1.38)

Heterogeneity between 3 groups χ^2_2= 2.3; P=.32

* 95% CI

Figure 2

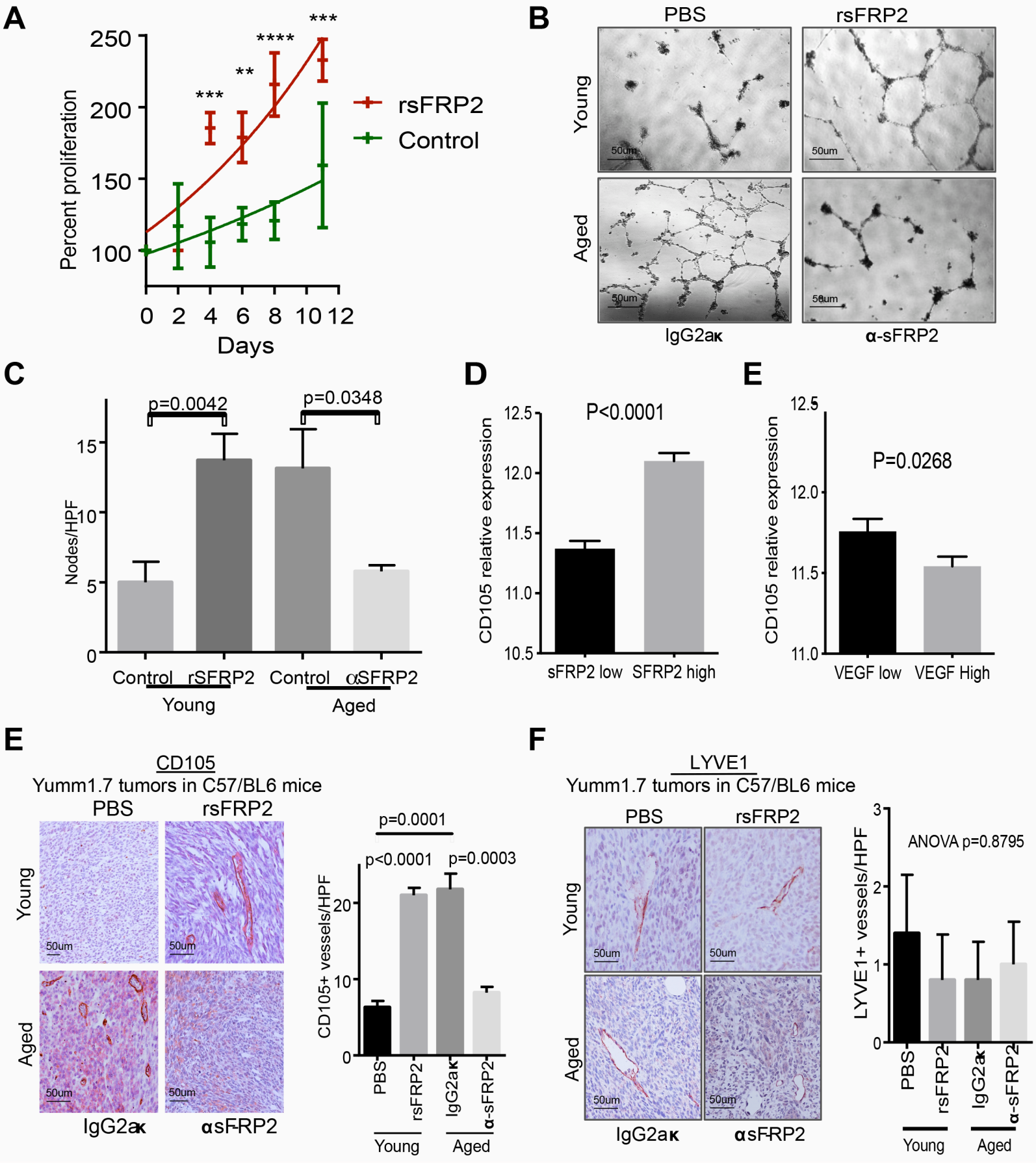
A
Percent proliferation
250
200
150
100
0 2 4 6 8 10 12
Days
***
**
****
***
rsFRP2
Control
B
PBS
rsFRP2
Young
Aged
50um
IgG2aκ
α-sFRP2
C
p=0.0042
p=0.0348
Nodes/HPF
15
10
5
0
Control rSFRP2 Control αSFRP2
Young
Aged
D
P<0.0001
CD105 relative expression
12.5
12.0
11.5
11.0
10.5
sFRP2 low SFRP2 high
E
P=0.0268
CD105 relative expression
12.5
12.0
11.5
11.0
VEGF low VEGF High
E
CD105
Yumm1.7 tumors in C57/BL6 mice
PBS
rsFRP2
Young
Aged
50um
IgG2aκ
αsFRP2
p=0.0001
p<0.0001
p=0.0003
CD105+ vessels/HPF
20
10
0
PBS
rsFRP2
IgG2aκ
α-sFRP2
Young
Aged
F
LYVE1
Yumm1.7 tumors in C57/BL6 mice
PBS
rsFRP2
Young
Aged
50um
IgG2aκ
αsFRP2
ANOVA p=0.8795
LYVE1+ vessels/HPF
3
2
1
0
PBS
rsFRP2
IgG2aκ
α-sFRP2
Young
Aged

Figure 3

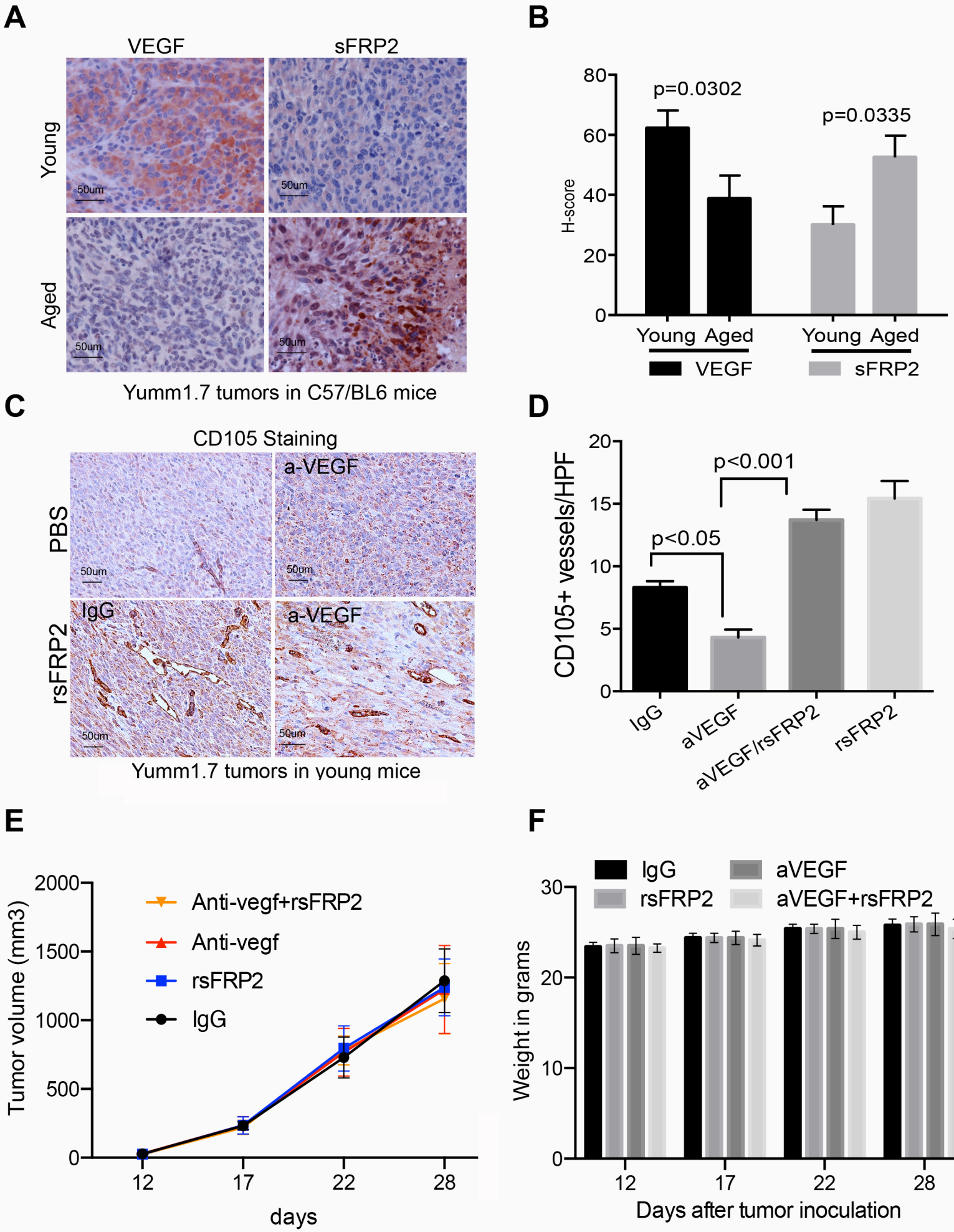
A
VEGF
sFRP2
Young
Aged
50um
Yumm1.7 tumors in C57/BL6 mice
B
H-score
p=0.0302
p=0.0335
Young Aged
Young Aged
VEGF
sFRP2
C
CD105 Staining
PBS
rsFRP2
a-VEGF
IgG
Yumm1.7 tumors in young mice
D
CD105+ vessels/HPF
p<0.001
p<0.05
IgG
aVEGF
aVEGF/rsFRP2
rsFRP2
E
Tumor volume (mm3)
Anti-vegf+rsFRP2
Anti-vegf
rsFRP2
IgG
days
F
IgG
aVEGF
rsFRP2
aVEGF+rsFRP2
Weight in grams
Days after tumor inoculation

Figure 4